ЖЭТФ, 2015, том 148, вып. 3 (9), стр. 573–583

NONEQUILIBRIUM KINETICS OF THE ELECTRON–PHONON SUBSYSTEM OF A CRYSTAL IN A STRONG ELECTRIC FIELD AS A BASE OF THE ELECTROPLASTIC EFFECT

V. I. Karas [a,b*], ***A. M. Vlasenko*** [a], ***V. I. Sokolenko*** [a], ***V. E. Zakharov*** [c,d]

[a] *National Science Center "Kharkov Institute of Physics and Technology", National Academy of Sciences of Ukraine 61108, Kharkov, Ukraine*

[b] *Karazin Kharkov National University 61022, Kharkov, Ukraine*

[c] *Lebedev Physical Institute, Russian Academy of Sciences 119991, Moscow, Russia*

[d] *Landau Institute for Theoretical Physics, Russian Academy of Sciences 142432, Chernogolovka, Moscow Region, Russia*

Received December 25, 2014

We present the results of a kinetic analysis of nonequilibrium dynamics of the electron–phonon system of a crystal in a strong electric field based on the proposed method of numerically solving a set of Boltzmann equations for electron and phonon distribution functions without expanding the electron distribution function in a series in the phonon energy. It is shown that the electric field action excites the electron subsystem, which by transferring energy to the phonon subsystem creates a large amount of short-wave phonons that effectively influence the lattice defects (point, lines, boundaries of different phases), which results in a redistribution of and decrease in the lattice defect density, in damage healing, in a decrease in the local peak stress, and a decrease in the degradation level of the construction material properties.

DOI: 10.7868/S004445101509014X

1. INTRODUCTION

In the 1960s, the phenomenon of an abrupt decrease in the plastic deformation resistance of metals in the case of excitation of their conductivity electron subsystem by irradiation or conduction of the electron current of a high density $j = 10^8$–10^9 A/m^2 was discovered. This phenomenon has been called the electroplastic effect (EPE) [1]. This effect is already being applied in industry in the processes of drawing and rolling metallic products.

Since then, Soviet and American scientists have carried out a series of experiments on metal deformation under the effect on electric current and also under irradiation of samples by accelerated electrons. In that experiments, manifestation of the EPE under different conditions was studied and also the dependence of the phenomenon intensity was ascertained on parameters such as:

– kind of the sample being deformed,
– temperature,
– current density amplitude,
– current pulse frequency,
– current pulse duration,
– current direction,
– dopant concentration in the sample,
– orientation of crystal samples being deformed,
– deformation rate.

Constructing an ab initio theory of the EPE is complicated because explaning the results of experiments on crystal deformation under the influence of electric current requires taking different mechanisms of the current influence on the deformation processes into account. These mechanisms include:

– thermic influence of the current, resulting in thermal expansion of the sample and also in softening,
– skin effect,

*E-mail: karas@kipt.kharkov.ua

– pinch effect, i. e., the influence of the pressure of the magnetic field created by the current inside the sample,

– electron–dislocation interaction that appears in the momentum and energy transfer to dislocations from both the electrons and collective excitations such as plasmons,

– phonon mechanism: the electrons that gain energy from the electric field create phonons that excite dislocation vibrations, which can result in the dislocation depinning from stoppers.

We enumerate some experimental regularities of the EPE.

In its purest state, the EPE can be observed in monocrystals of Zn, Cd, Sn, and Pb. If pulsed electric current with the density $j = 10^2$–10^3 A/mm^2 is passed through a sample of these materials, or if the samples are irradiated by accelerated electrons (with the energy less than the atomic knock-out threshold from the lattice node) in the slip direction, then softening of the samples is revealed, manifesting itself in spasmodic drops of deforming stress [1].

For monocrystals, a strongly expressed dependence of the effect magnitude on the orientation of the samples being deformed is observed. At the crystal orientations such that the basal slip is complicated, the magnitude of the deforming stress drop if small and the stress from which plastic deformation begins is large. The maximum stress drop magnitude can be obtained for medium crystal orientations that are characterized by an easy basal slip. In this case, the stress of the drop start has its minimum [1].

The EPE magnitude dependence on the current density has a threshold character, i. e., it becomes apparent at a particular value of the pulsed current density. This value depends on the sort of crystals being deformed and also on the temperature and on the deformation rate. For zinc at $T = 77$ K, it is equal to 400–500 A/mm^2 [1].

The temperature dependence is almost absent in a wide range of temperatures. For zinc, this range is 77–300 K. For titan, the threshold current density magnitude from which the effect begins with cooling from 300 to 78 K increases by hundreds of A/cm^2 [1]. The EPE is sensitive to external factors. The effect intensity is influenced by surface-active media. For example, the specific crystallographic shift of amalgamated zinc monocrystals at the temperature of 300 K and under the influence of current pulses with $j = 600$–1000 A/mm^2, the pulse repetition frequency 0.1–0.5 Hz, and the pulse duration $t_p = 10^{-4}$ s increases by 50–60 % [1].

The dopant presence also affects the spasmodic metal deformation. As a result of doping, the drop magnitude can increase by dozens of percents (up to 100 %). Within the scope of a relatively small substitutional impurity, the magnitude of the effect increases linearly with the concentration, as has been shown in the experiments with zinc doped by cadmium from 10^{-3} to 10^{-1} at. % (other impurities content did not exceed $2 \cdot 10^{-3}$ at. %). The brittle strength of zinc crystals increases by 50–70 % depending on the dopant concentration. This fact can be connected with the general increase in the critical shearing stress in doped crystals [1]. The increase in the current pulse repetition frequency decreases the deforming stress threshold value but also decreases the stress drop magnitude. The pulse duration increase at constant amplitude increases the depth of stress drops. This phenomenon was registered both in stress relaxation tests and in creep tests [1].

The main EPE regularities, revealed at monocrystal deformation, can be observed in a weaker form also in experiments with polycrystal materials. However, the EPE magnitude decreases with structure refinement and even disappears in the nanocrystal state [2]. Hence, the EPE is a structure-sensitive phenomenon. Similar phenomena are observed under irradiation of the material by pulse packets of accelerated electrons. Plasticizing action enhances with the increase in the electron energy to the atomic knockout threshold. Under a further energy increase, the intensity of the effect decreases at the expense of radiation strengthening. The combination of current action and irradiation results in the intensification of the metal strength loss effect [1].

The mechanisms connected with the action of electron wind on dislocations, pinch effect, and thermal influence of the current on deformation processes are reviewed in detail in [1]. It is shown that they are not sufficient for a quantitative explanation of the EPE. In this paper, the phonon mechanism of the influence on dislocation is considered (see [3, 4]). Some preliminary results of such studies were reported at the International Conference MSS-14 "Mode Conversion, Coherent Structures, and Turbulence" (November 24–27, 2014, Moscow) and were also published in the conference proceedings [5, 6].

The purpose of this paper is to show that the experimentally observed regularities of the electroplastic effect can be explained quantitatively if we take into account the influence of nonequilibrium phonons excited by electrons that gain energy from the electric field on the dislocations.

2. THE INFLUENCE OF PHONONS ON DISLOCATIONS

Plastic deformation of crystals under the action of external loads is in most cases accomplished by dislocation glide. The main equation describing the kinetics of the plastic deformation process is the Orovan modified equation (see, e. g., [7])

$$\dot{\varepsilon}_d = bl\rho_d\nu_d(\sigma^*), \quad \sigma^* = \sigma - \sigma_i, \tag{1}$$

where $\dot{\varepsilon}_d$ is the strain rate, b is Burgers vector, l is the mean distance between stoppers, ρ_d is the mobile dislocations density, $\nu_d(\sigma^*)$ is the frequency of the stoppers overcome by dislocations, σ^* is the effective shear stress, and σ_i is the internal shearing stress in the glide plane. For thermodynamic equilibrium, the expression $\nu_d(\sigma^*, T)$ has the form

$$\nu_d(\sigma^*, T) = \nu_d^0 \exp\left(-\frac{H(\sigma^*)}{k_B T}\right), \tag{2}$$

where k_B is the Boltzmann constant and T is the temperature. The explicit form of the $H(\sigma^*)$ function depends on the potential barrier model. To consider a more general case where the electron and phonon subsystems are not in equilibrium in general, we use the Landau–Hoffman model [8]. The potential pit has a parabolic form,

$$U(x) = \begin{cases} \zeta x^2, & |x| \le x_{cr}, \\ 0, & |x| > x_{cr}, \end{cases} \qquad \zeta x_{cr}^2 = U_0. \tag{3}$$

The displacement of the dislocation segment of length L under the stress σ is described in the approximation of elastic string vibrations (the Granato–Lücke model [8, 9]):

$$M\frac{\partial^2 u}{\partial t^2} + B\frac{\partial u}{\partial t} - C\frac{\partial^2 u}{\partial y^2} = b\sigma + f(t). \tag{4}$$

Here, $u(y,t)$ is the displacement of the dislocation line at a point y in the direction x, $M = \rho b^2/2$ is the effective mass of the length unit, ρ is the material density, B is the coefficient of the dynamic friction force per unit length, $C = Gb^2/2$ is the linear tension of the string, G is the shear modulus, and $f(t)$ is the force of the random pushes exerted by the crystal on the unit dislocation length. The boundary conditions are

$$u'(0,t) = ku(0,t), \quad -u'(L,t) = ku(L,t), \qquad k = \frac{2\zeta}{C}. \tag{5}$$

The equation is linear, and therefore its solution can be written as a sum

$$u(y,t) = u_{st}(y) + u_{osc}(y,t),$$

where $u_{st}(y)$ is the static deflection caused by the external stress σ, and $u_{osc}(y,t)$ stands for the oscillations under the action of a random force:

$$u_{st}(y) = \frac{by(L-y)}{2C} + \frac{bL\sigma}{2Ck},$$
$$u_{osc}(y,t) = \sum_{n=1}^{N} Q_n(t)\left(\sin(q_n y) + \frac{q_n}{k}\cos(q_n y)\right), \tag{6}$$
$$\operatorname{ctg}(q_n y) = \frac{q_n^2 - k^2}{2q_n k}.$$

The quantity $Q_n(t)$ satisfies the equation

$$M\ddot{Q}_n(t) + B\dot{Q}_n(t) + M\omega_n^2 Q_n(t) = f_n(t), \qquad \omega_n^2 = q_n^2\frac{C}{M}. \tag{7}$$

We consider a "fixing point" at $y = 0$. Let the segment lengths on both sides of it be equal to L. Then the total deflection at the "fixing point" is

$$\tilde{u}(0,t) = 2u_{st}(y) + 2u_{osc}(y,t) = \tilde{u}_{st}(y) + \tilde{u}_{osc}(y,t). \tag{8}$$

The case of a random force was considered in [10]. We now provide some of the calculations for the reference purpose. If a random event such that $\delta\tilde{u}(0,t) \ge \delta\tilde{u}_{cr}$ occurs at some instant, then the condition of overcoming the obstacle in the direction on the loading action is satisfied. Let $f_n(t)$ be a stationary Gauss process. Because Eq. (7) is linear, $Q_n(t)$ and accordingly $\tilde{u}(0,t)$ is also a stationary Gauss process, for which the mean number of the instances of exceeding a particular value $\delta\tilde{u}_{cr}$ per unit time is

$$\nu = \frac{1}{2\pi}\sqrt{-\frac{\Psi''(0)}{\Psi(0)}}\,\exp\left\{-\frac{\delta\tilde{u}_{cr}^2}{2\Psi(0)}\right\}, \tag{9}$$

$$\Psi(\tau) = 2\sum_{n=1}^{\bar{n}}\frac{q_n^2}{k^2}\overline{Q_n(t)Q_n(t+\tau)} \equiv 2\sum_{n=1}^{\bar{n}}\frac{q_n^2}{k^2}\psi(\tau), \tag{10}$$

$$\delta\tilde{u}_{cr} = x_{cr} - \frac{bL\sigma}{Ck} = x_{cr}\left(1 - \frac{\sigma}{\sigma_{cr}}\right), \qquad \sigma_{cr} \equiv \frac{Ckx_{cr}}{bL}, \tag{11}$$

where $\Psi(\tau)$ is the correlation function of the random process $\delta\tilde{u}(0,t)$ expressed by means of the correlation function $\psi(\tau)$ of the random process $Q_n(t)$; $\Psi''(0)$ is the second derivative with respect to τ at $\tau = 0$. For the Fourier components $(Q_n)_\omega$ of $Q_n(t)$, we can write

$$\psi(\tau) = \int_{-\infty}^{\infty}(Q_n)_\omega^2 e^{-i\omega\tau}\,d\omega, \tag{12}$$

where $(Q_n)_\omega^2$ is defined by the relation

$$\overline{(Q_n)_\omega (Q_n)_{\omega'}} = (Q_n)_\omega^2 \delta(\omega + \omega'). \tag{13}$$

Each harmonic can be formally considered an independent vibrator with the friction χ and frequency ω_n,

$$m\ddot{Q} + \chi\dot{Q} + m\omega_n^2 Q = F, \tag{14}$$

where m is the proportionality coefficient between the generalized momentum and the velocity $\dot{Q}$, χ is the friction coefficient, and F is the random force [11]. We have

$$m = M\frac{L\xi_n}{2}, \quad \chi = B\frac{L\xi_n}{2}, \quad F = f_n\frac{L\xi_n}{2}, \qquad \xi_n = 1 - \frac{2}{kL} + \frac{q_n^2}{k^2}. \tag{15}$$

For the Fourier component, we hence obtain the formula

$$(Q_n)_\omega^2 = \frac{(F_\omega)^2}{m^2(\omega_n^2 - \omega^2)^2 + \chi^2\omega^2}. \tag{16}$$

The random force spectral density can be found from the expression [8]

$$(F_\omega)^2 = \frac{\chi}{\pi}\hbar\omega\left(\frac{1}{2} + N(\omega)\right). \tag{17}$$

Hence, to estimate the force exerted by phonons on dislocations, we must first find the phonon distribution function $N(\omega)$.

3. KINETIC EQUATIONS

In some works on the electron–phonon subsystem dynamics in metal films, an assumption about the Fermi form of the isotropic part of the electron distribution function with time-dependent temperature was used [12]. Here, we do not make that assumption, and therefore the distribution functions can be not thermodynamically equilibrium in general. In that case, the behavior of electrons and phonons is described by means of distribution functions.

To describe the electron–phonon system nonequilibrium dynamics, it is necessary to solve a set of kinetic Boltzmann equations for the electron and phonon distribution functions. For the electron distribution function, the Boltzmann equation has the form

$$\frac{\partial f}{\partial t} + \boldsymbol{\nu}\frac{\partial f}{\partial \mathbf{r}} + \frac{\partial f}{\partial \mathbf{p}}\frac{d\mathbf{p}}{dt} = I_{ee} + I_{ep} + I_{ed}, \tag{18}$$

$$\frac{d\mathbf{p}}{dt} = e\mathbf{E}(\mathbf{r}, t), \tag{19}$$

where $\boldsymbol{\nu}$ is the velocity, $\mathbf{p}$ is the momentum, t is time, $\mathbf{r}$ is the radius vector, $\mathbf{E}$ is the electric field strength, and e is the electron charge. Here and hereafter, we assume that the magnetic field is absent. We assume that the electric field and the electron and phonon distribution functions are spatially uniform and that the electron distribution function isotropization occurs as a result of electron–defect collisions. In this case, we can neglect the umklapp processes.

In (18), I_{ee} is the electron–electron collision integral. In the general case of quantum mechanics, it has the form [13–15]

$$I_{ee} = \frac{2}{(2\pi\hbar)^6}\int d\mathbf{p}_1 d\mathbf{p}_2 d\mathbf{p}_3 W(\mathbf{p}, \mathbf{p}_1|\mathbf{p}_2, \mathbf{p}_3) \times \\ \times [f(\mathbf{p}_2)f(\mathbf{p}_3)(1 - f(\mathbf{p}_1))(1 - f(\mathbf{p})) - \\ - f(\mathbf{p})f(\mathbf{p}_1)(1 - f(\mathbf{p}_2))(1 - f(\mathbf{p}_3))] \times \\ \times \delta(\varepsilon + \varepsilon_1 - \varepsilon_2 - \varepsilon_3)\delta(\mathbf{p} + \mathbf{p}_1 - \mathbf{p}_2 - \mathbf{p}_3), \tag{20}$$

where $f(\mathbf{p})$ are the occupation numbers and

$$W(\mathbf{p}, \mathbf{p}_1|\mathbf{p}_2, \mathbf{p}_3) = (2\pi\hbar)^3 2e^4\left(|\mathbf{p}_1 - \mathbf{p}_3|^2 + a_1^2\right)^{-2} \tag{21}$$

is the matrix element that describes the screened coulomb interaction, where $W(\mathbf{p}, \mathbf{p}_1|\mathbf{p}_2, \mathbf{p}_3)$ is the transition probability for electrons with momenta $\mathbf{p}_2$ and $\mathbf{p}_3$ to the state with momenta $\mathbf{p}$ and $\mathbf{p}_1$ as a result of collision. For relatively small electric fields, the contribution from electron–electron collisions is much less than the contribution from the electron–phonon interaction, and we therefore do not take the electron–electron collisions at short time intervals into account in what follows. As was shown in [4], the role of the electron–electron collision integral amounts to a redistribution of the energy acquired by electrons from the electric field. The lower estimate for the characteristic electron–electron relaxation time can be obtained from the heat balance equation

$$\frac{E^2}{\rho_S}\tau_{ee} = \rho c_p \delta T$$

and it turns out to be greater than the characteristic time of the electron–phonon relaxation. Here, E is the electric field intensity, ρ_S is the specific residual resistance measured in experiment ($3 \cdot 10^{-8}$ Ohm $\cdot$ m, while the specific resistance caused by the electron–phonon collisions is several orders less), c_p is the specific heat capacity at constant pressure (in our case, it is approximately equal to 25 J$\cdot$kg$^{-1}\cdot$K^{-1}), ρ is the density of our material, δT is the increase in temperature, which is comparable to our initial temperature, and I_{ep} is the electron–phonon collision integral [13–15]:

$$I_{ep} = \int d\mathbf{q}\, w(\mathbf{q}) \{\delta\left(\varepsilon(\mathbf{p}+\mathbf{q}) - \varepsilon(\mathbf{p}) - \hbar\Omega(\mathbf{q})\right) \times$$
$$\times \left[f(\mathbf{p}+\mathbf{q})\left(1-f(\mathbf{p})\right)\left(N(\mathbf{q})+1\right) - \right.$$
$$\left. - f(\mathbf{p})\left(1-f(\mathbf{p}+\mathbf{q})\right)N(\mathbf{q})\right] +$$
$$+ \delta\left(\varepsilon(\mathbf{p}-\mathbf{q}) - \varepsilon(\mathbf{p}) + \hbar\Omega(\mathbf{q})\right) \times$$
$$\times \left[f(\mathbf{p}-\mathbf{q})\left(1-f(\mathbf{p})\right)N(\mathbf{q}) - f(\mathbf{p}) \times \right.$$
$$\left. \times \left(1-f(\mathbf{p}-\mathbf{q})\right)\left(N(\mathbf{q})+1\right)\right]\}. \quad (22)$$

Next, I_{ed} is the electron–impurity and electron–defect collision integral. It can be obtained by setting $\hbar\Omega = 0$ and $N = 0$ in I_{ep}:

$$I_{ed} = \int d\mathbf{p}'\, w_{ed}(\mathbf{p}'-\mathbf{p})\delta\left(\varepsilon(\mathbf{p}') - \varepsilon(\mathbf{p})\right) \times$$
$$\times \{f(\mathbf{p}') - f(\mathbf{p})\}. \quad (23)$$

The phonon distribution function also satisfies the kinetic equation

$$\frac{\partial N(\mathbf{q})}{\partial t} + \boldsymbol{\nu}_q \frac{\partial N(\mathbf{q})}{\partial \mathbf{r}} = I_{pe} + I_{pp} + I_{pd}, \quad (24)$$

where I_{pe} is the phonon–electron collision integral [13–15]

$$I_{pe} = \int d\mathbf{p}\, w(\mathbf{q}) \{\delta\left(\varepsilon(\mathbf{p}+\mathbf{q}) - \varepsilon(\mathbf{p}) - \hbar\Omega(\mathbf{q})\right) \times$$
$$\times \left[f(\mathbf{p}+\mathbf{q})\left(1-f(\mathbf{p})\right)\left(N(\mathbf{q})+1\right)\right] -$$
$$- f(\mathbf{p})\left(1-f(\mathbf{p}+\mathbf{q})\right)N(\mathbf{q})\}. \quad (25)$$

The phonon–phonon and phonon–defect collision integrals in the τ-approximation have the following form. The phonon–phonon collision integral is

$$I_{pp} = -\nu_{pp}(\mathbf{q})\left[N(\mathbf{q}) - N_T(\mathbf{q})\right],$$
$$\nu_{pp}(q) = \nu_{pp0}q^2, \quad \nu_{pp0} = \frac{T^3 s}{aT_D^4 M_c}, \quad (26)$$

where s is the transverse sound velocity, M_c is the atom mass, a is the lattice constant, and T_D is the Debye temperature. The phonon–defect collision integral is

$$I_{pd} = -\nu_{pd}(\mathbf{q})\left[N(\mathbf{q}) - \overline{N(\mathbf{q})}\right], \quad (27)$$

where

$$N_T(\mathbf{q}) = \left(\exp\frac{\hbar\Omega}{T} - 1\right)^{-1}$$

is the thermodynamically equilibrium phonon distribution function (the Bose–Einstein function), and

$$\overline{N}(q) = \frac{1}{4\pi}\int N(\mathbf{q})\, dO$$

is the phonon distribution function averaged over angles.

Because the electron–impurity, electron–defect, and electron–phonon collisions result in the distribution function isotropization, we seek it in the form of a sum of an isotropic function and a small anisotropic addition:

$$f(\mathbf{p},\mathbf{t}) = f\left(\varepsilon(p),t\right) + \mathbf{f}_1\left(\varepsilon(p),t\right)\frac{\mathbf{p}}{p}, \quad (28)$$

$$w(q) = w_0 q, \quad w_0 = \frac{\varepsilon_{1A}^2}{2(2\pi\hbar)^2\hbar\rho s}, \quad \hbar\Omega(q) = sq, \quad (29)$$

where ε_{1A} is the deformation potential constant, which in our particular model case is equal to $2\varepsilon_F/3$, with ε_F being the Fermi energy. We finally obtain

$$I_{pp} = -\nu_{pd0}q\left[N(\mathbf{q}) - N_T(\mathbf{q})\right], \quad (30)$$

$$I_{ed}\left\{\mathbf{f}_1(\varepsilon)\frac{\mathbf{p}}{p}\right\} = -\nu_{ed}\mathbf{f}_1(\varepsilon)\frac{\mathbf{p}}{p}, \quad \nu_{ed} = \frac{\rho_s n e^2}{m}, \quad (31)$$

where m is the effective electron mass and $\nu_{ed} = 3\cdot 10^{13}$ s^{-1} is the electron–impurity collision frequency, which in the given case (of low temperatures) determines the electron distribution function isotropization. Also,

$$I_{ep}\left\{\mathbf{f}_1(\varepsilon)\frac{\mathbf{p}}{p}\right\} = -\nu(\varepsilon)\mathbf{f}_1(\varepsilon)\frac{\mathbf{p}}{p},$$
$$\nu(\varepsilon) = \frac{\pi w_0}{\sqrt{m\varepsilon^3}}\int_0^{\sqrt{8m\varepsilon}} dq\, q^3\left[N(q) + \frac{1}{2}\right]. \quad (32)$$

For the anisotropic addition, we have the equation

$$\frac{\partial \mathbf{f}_1}{\partial t}\frac{\mathbf{p}}{p} - e\mathbf{E}\nu\frac{\partial f_0}{\partial\varepsilon}\frac{\mathbf{p}}{p} = -\nu_{ed}\mathbf{f}_1(\varepsilon)\frac{\mathbf{p}}{p}. \quad (33)$$

The electron–phonon collision frequency $\nu_{ep} = 1.18 \times 10^{10}$ s^{-1} is much less than the electron–defect collision frequency. Collisions with defects and impurities occur very often, at a time scale that is small compared to the characteristic time of the interaction of phonons with electrons, and therefore the anisotropic addition can be considered stationary and spatially uniform. For this statement to be true, the impurity concentration must be much greater than the concentration at which the electron–defect collision frequency is equal to the electron–phonon collision frequency. In our case, this concentration has to be greater than $1.77\cdot 10^{17}$ cm^{-3}, that is, several orders less than for the considered experiments. As a result, we obtain the final set of two equations for the isotropic electron and acoustic phonon distribution functions [3, 4, 16], which has to be solved without expanding the electron distribution function in a Taylor series:

$$\frac{\partial f}{\partial \tilde{t}} - 4\Delta\tilde{\varepsilon}\frac{1}{\tilde{\varepsilon}^{1/2}}\frac{\partial}{\partial\tilde{\varepsilon}}\left[\tilde{\varepsilon}^{3/2}\frac{\partial f}{\partial\tilde{\varepsilon}}\right] = \frac{1}{8}\,\alpha^{-5/2}\times$$
$$\times\left\{\frac{1}{\sqrt{\tilde{\varepsilon}}}\int\limits_{\sqrt{\tilde{\varepsilon}}}^{\varepsilon_-} d\tilde{\varepsilon}_{ph}\tilde{\varepsilon}_{ph}^2\left[f\left(\tilde{\varepsilon}-\tilde{\varepsilon}_{ph}\right)N(\tilde{\varepsilon}_{ph})\;+\right.\right.$$
$$+\;f(\tilde{\varepsilon})\left(f(\tilde{\varepsilon}-\tilde{\varepsilon}_{ph})-N(\tilde{\varepsilon}_{ph})-1\right)\Big] +$$
$$+\frac{1}{\sqrt{\tilde{\varepsilon}}}\int\limits_0^{\varepsilon_+} d\tilde{\varepsilon}_{ph}\tilde{\varepsilon}_{ph}^2\left[f\left(\tilde{\varepsilon}+\tilde{\varepsilon}_{ph}\right)\left(N(\tilde{\varepsilon}_{ph})+1\right)-\right.$$
$$\left.\left.-\;f(\tilde{\varepsilon})\left(f\left(\tilde{\varepsilon}+\tilde{\varepsilon}_{ph}\right)+N(\tilde{\varepsilon}_{ph})\right)\right]\right\}, \quad (34)$$

$$\frac{\partial N(q)}{\partial\tilde{t}} = \frac{1}{2\alpha}\int\limits_{\varepsilon_0}^{\infty} d\tilde{\varepsilon}\left[\left(f(\tilde{\varepsilon}+\tilde{\varepsilon}_{ph})-f(\tilde{\varepsilon})\right)N(\tilde{\varepsilon}_{ph})\;+\right.$$
$$\left.+\;f(\tilde{\varepsilon}+\tilde{\varepsilon}_{ph})\left(1-f(\tilde{\varepsilon})\right)\right]. \quad (35)$$

Here,

$$\alpha = \frac{ms^2}{2k_BT_e}, \quad \Delta\tilde{\varepsilon} = \frac{e^2E^2\tau_{ep0}}{6m\nu_{ed}k_BT_e}, \quad \tilde{\varepsilon} = \frac{\varepsilon}{k_BT_e},$$
$$\tilde{\varepsilon}_{ph} = \frac{\varepsilon_{ph}}{k_BT_e}, \quad \tilde{t} = \frac{t}{\tau_{ep0}},$$
$$\tau_{ep0} = \frac{(2\pi\hbar)^3\hbar\rho}{\pi m^3 s\varepsilon_{1A}^2} = 3.446\cdot10^{-7}\ \text{s}.$$

The integration limits, which are obtained in accordance with the energy conservation law, are

$$\varepsilon_- = \min\left[4\left(\sqrt{\tilde{\varepsilon}}\alpha-\alpha\right),\tilde{\varepsilon}_{ph_D}\right],$$
$$\varepsilon_+ = \min\left[4\left(\sqrt{\tilde{\varepsilon}}\alpha+\alpha\right),\tilde{\varepsilon}_{ph_D}\right], \quad (36)$$
$$\varepsilon_0 = \frac{\tilde{\varepsilon}_{ph}^2}{16\alpha} - \frac{\tilde{\varepsilon}_{ph}}{2} + \alpha.$$

The distribution functions of electrons $f(\varepsilon)$ and phonons $N(q)$ are dimensionless quantities that satisfy the normalization conditions

$$\frac{1}{2\pi^2}\left(\frac{2m}{\hbar^2}\right)^{3/2}\int\limits_0^{\infty}\varepsilon^{1/2}f(\varepsilon)\,d\varepsilon = n, \quad (37)$$

where n is the electron density in the valence band (for metals, also the conductivity band, because it is only partially filled),

$$\frac{1}{2\pi^2}\,\frac{1}{\hbar^3}\int\limits_0^{q_D} q^2N(q)\,dq < \infty, \quad (38)$$

where

$$q_D = \frac{\pi\hbar}{a} \quad (39)$$

is the Debye phonon momentum. Condition (38) expresses the fact that the number of phonons does not have to be conserved. All quantities are taken for nickel: $s = 2.96\cdot10^5$ cm/s is the transverse sound velocity, $n = 2.5\cdot10^{22}$ cm^{-3} is the conductivity electron concentration, $a = 3.5\cdot10^{-8}$ cm, and $\rho_s^{-1} = 0.333\cdot10^6$ S/cm.

The thermodynamically equilibrium electron energy distribution function is the Fermi–Dirac function

$$f_0(\varepsilon) = \left(\exp\frac{\varepsilon-\varepsilon_F}{k_bT_e}+1\right)^{-1}. \quad (40)$$

For nickel, $\varepsilon_F = 5\cdot10^{-19}$ J.

4. NUMERICAL SOLUTION OF THE SET OF KINETIC EQUATIONS FOR ELECTRON AND PHONON DISTRIBUTION FUNCTIONS

For the numerical solution of Eqs. (34), (35), the finite-difference method of the first-order approximation over time and second-order over spatial coordinates was used. System (34), (35) was represented by the following set of difference equations [17]:

$$\frac{f_i^{\nu+1}-f_i^{\nu}}{\tilde{\tau}} = 6\Delta\tilde{\varepsilon}\frac{f_{i+1}^{\nu+1}-f_{i-1}^{\nu+1}}{2\hbar_{\tilde{\varepsilon}}} +$$
$$+\,4\tilde{\varepsilon}_i\Delta\tilde{\varepsilon}\frac{f_{i+1}^{\nu+1}-2f_i^{\nu+1}+f_{i-1}^{\nu+1}}{\hbar_{\tilde{\varepsilon}}^2} + J_i, \quad (41)$$

$$J_i = \frac{1}{8\sqrt{\tilde{\varepsilon}_i\alpha^5}}\,\frac{1}{2}\left\{\sum_{j=0}h_{\tilde{\varepsilon}_{ph}}\tilde{\varepsilon}_{ph_j}^2\times\right.$$
$$\times\left[f_k^{\nu}N_j + f_i^{\nu}(f_k^{\nu}-N_j-1)\right] +$$
$$+\sum_{j=0}h_{\tilde{\varepsilon}_{ph}}\tilde{\varepsilon}_{ph_j}^2\left[f_l^{\nu}(N_j+1)-f_l^{\nu}(f_l^{\nu}+N_j)\right] +$$
$$+\sum_{j=0}h_{\tilde{\varepsilon}_{ph}}\tilde{\varepsilon}_{ph_{j+1}}^2\left[f_{k-1}^{\nu}N_{j+1}+f_i^{\nu}(f_{k-1}^{\nu}-N_{j+1}-1)\right] +$$
$$+\sum_{j=0}h_{\tilde{\varepsilon}_{ph}}\tilde{\varepsilon}_{ph_{j+1}}^2\left[f_{l+1}^{\nu}(N_{j+1}+1)-\right.$$
$$\left.\left.-\;f_i^{\nu}(f_{l+1}^{\nu}+N_{j+1})\right]\right\}, \quad (42)$$

$$\frac{N_j^{\nu+1}-N_j^{\nu}}{\tilde{\tau}} = \frac{1}{2\alpha}\,\frac{1}{2}\sum_i h_{\tilde{\varepsilon}}\left[(f_k^{\nu}-f_i^{\nu})N_j^{\nu}\;+\right.$$
$$\left.+\,f_k^{\nu}(1-f_i^{\nu})+(f_{k+1}^{\nu}-f_{i+1}^{\nu})N_j^{\nu}+f_{k+1}^{\nu}(1-f_{i+1}^{\nu})\right], \quad (43)$$

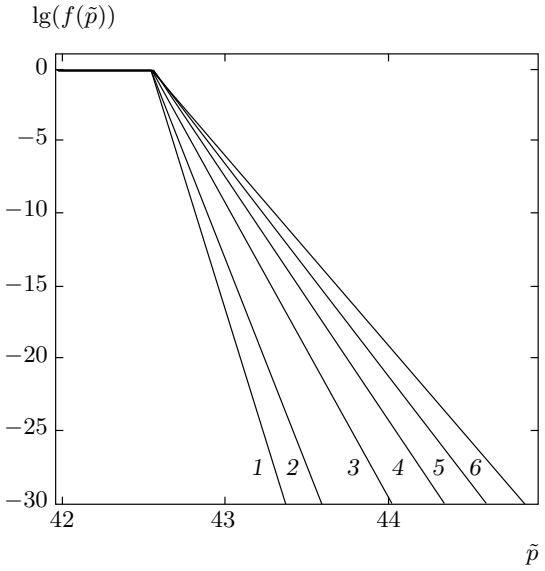

Fig. 1. Dependence of the electron distribution function decimal logarithm on the dimensionless electron momentum $\tilde{p}$ at $E = 1.68$ V/cm for different time instants $t = 0$ (*1*), 1 (*2*), 5 (*3*), 10 (*4*), 15 (*5*), 20 (*6*)

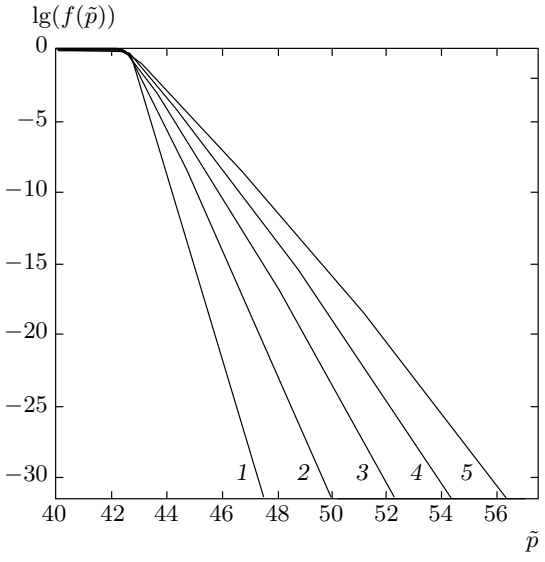

Fig. 2. Dependence of the electron distribution function decimal logarithm on the dimensionless electron momentum at $E = 33.6$ V/cm for different time instants $t = 0.25$ (*1*), 0.5 (*2*), 0.75 (*3*), 1 (*4*), 1.25 (*5*)

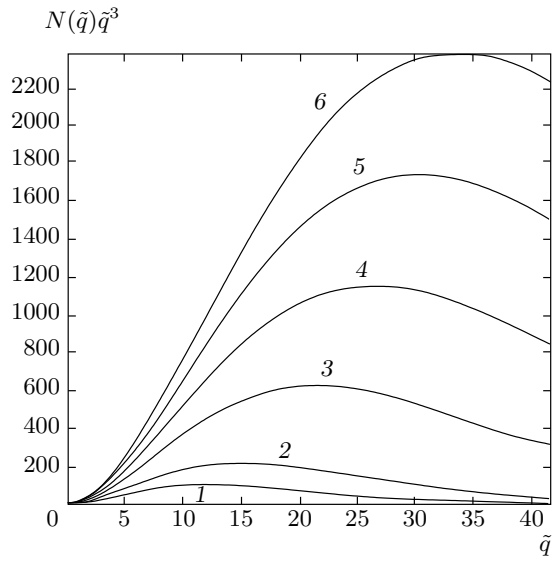

Fig. 3. Dependence of the phonon distribution function times the dimensionless phonon momentum $\tilde{q}$ cubed on the dimensionless phonon momentum at $E = 1.68$ V/cm for different time instants $t = 0$ (*1*), 1 (*2*), 5 (*3*), 10 (*4*), 15 (*5*), 20 (*6*)

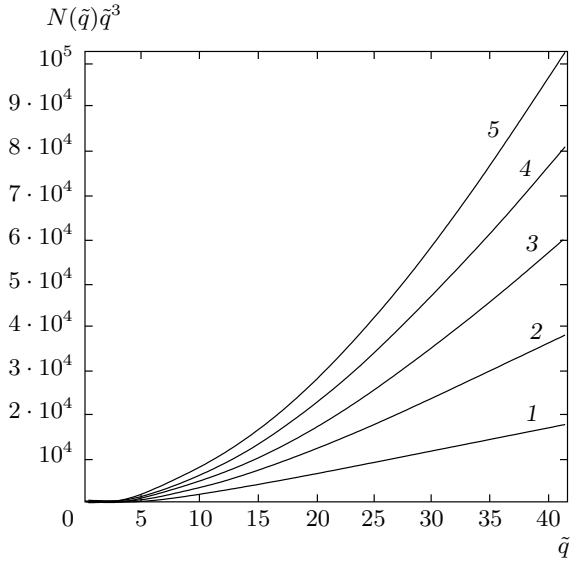

Fig. 4. Dependence of the phonon distribution function times the dimensionless phonon momentum cubed on the dimensionless phonon momentum at $E = 33.6$ V/cm for different time instants $t = 0.25$ (*1*), 0.5 (*2*), 0.75 (*3*), 1 (*4*), 1.25 (*5*)

$$f_k^{\nu} = f\left(\tilde{\varepsilon}_i - \tilde{\varepsilon}_{ph_j}\right), \quad f_l^{\nu} = f\left(\tilde{\varepsilon}_i + \tilde{\varepsilon}_{ph_j}\right). \tag{44}$$

The summation limits are determined from (26). Grid steps were chosen such that

$$\tilde{\varepsilon}_i - \tilde{\varepsilon}_{ph_j} = \tilde{\varepsilon}_k, \quad \tilde{\varepsilon}_i + \tilde{\varepsilon}_{ph_j} = \tilde{\varepsilon}_l, \tag{45}$$

where k and l are natural numbers. As a result of the calculations, the electron and phonon distribution functions were found.

In Fig. 1 and Fig. 2, we presented the dependence of

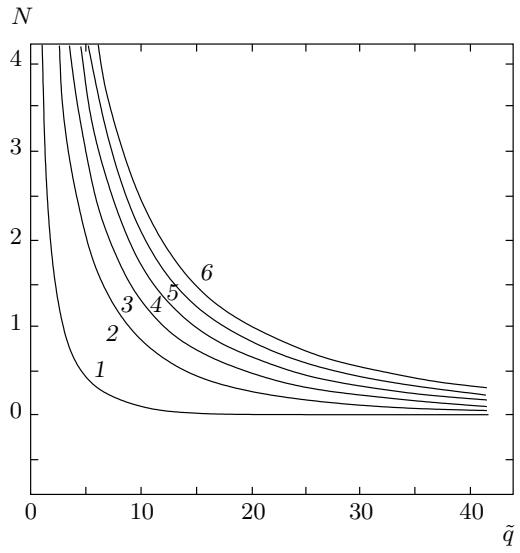

Fig. 5. Dependence of the phonon distribution function on the dimensionless phonon momentum at $E = 16.8$ V/cm for different time instants $t = 0$ (*1*), 0.25 (*2*), 0.5 (*3*), 0.75 (*4*), 1 (*5*), 1.25 (*6*)

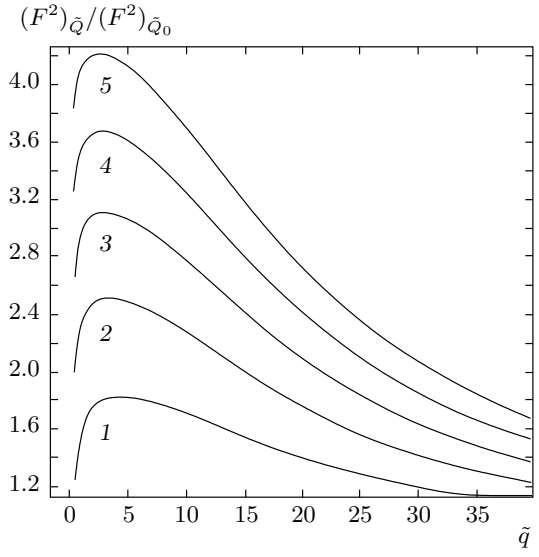

Fig. 6. Dependence of the ratio $(F_{\tilde{q}})^2/(F_{\tilde{q}_0})^2$ on the dimensionless phonon momentum for different time instants $t = 0.25$ (*1*), 0.5 (*2*), 0.75 (*3*), 1 (*4*), 1.25 (*5*) at $E = 16.8$ V/cm

the electron distribution function decimal logarithm on the dimensionless electron momentum for different time instants and two values of the electric field strength: 1.68 V/cm and 33.6 V/cm. In Figs. 3 and 4, we present the dependence of the phonon distribution function times the dimensionless phonon momentum cubed on the dimensionless momentum. The curves illustrate uninterrupted growth of the number of high-energy electrons and phonons with time. The curves for the instant $t = 0$ correspond to equilibrium distribution functions. In particular, the phonon distribution function times the dimensionless phonon momentum cubed for the electric field strength 33.6 V/cm at the instant ($t = 1.0$) of an order less than for the field 1.68 V/cm ($t = 10$) is more than 66 times greater. For the same values of t and of the electric field strengths, the values of the electron momentum at which the electron distribution function equals 10^{-30} differ by 1.23 times. Here, 10^{-30} is the value of the electron distribution function at which we terminate our grid. It does not have any specific meaning.

For clarity, in Fig. 5, we present a dependence of the phonon distribution function on the dimensionless momentum at the electric field strength $E = 16.8$ V/cm for different time instants.

To estimate the influence on the plastic deformation, we plot the dependence

$$\frac{(F_{\tilde{q}})^2}{(F_{\tilde{q}_0})^2} = \frac{1/2 + N(\tilde{q})}{1/2 + N_0(\tilde{q})}, \tag{46}$$

where $N_0(\tilde{q})$ is the Bose–Einstein function for the temperature 32 K, i. e., 12 K more than the initial temperature, and $N(\tilde{q})$ is the phonon distribution function found as a result of numerical calculations. For the most part, the heating in the experiments in [1] did not exceed 0.5–3 K.

From Fig. 6 and Fig. 7 we can see that the force exerted by phonons upon dislocation is greater than in case of simple heating and it has trend to grow with time.

5. COMPARISON WITH THE EXPERIMENTAL RESULTS

Figure 8 presents the dependence of the phonon distribution function times the dimensionless phonon momentum cubed on the dimensionless momentum in the double logarithmic scale for different situations:

- thermodynamic equilibrium phonon distribution functions at 20 K (curve *1*) and 32 K (curve *2*),
- the nonequilibrium phonon distribution function obtained as a result of numerical calculations at the electric field strength $E = 16.8$ V/cm for the instant $t = 2.5$ (curve *3*).

The value of the loading drop was found in the following order. First, we substitute the obtained values

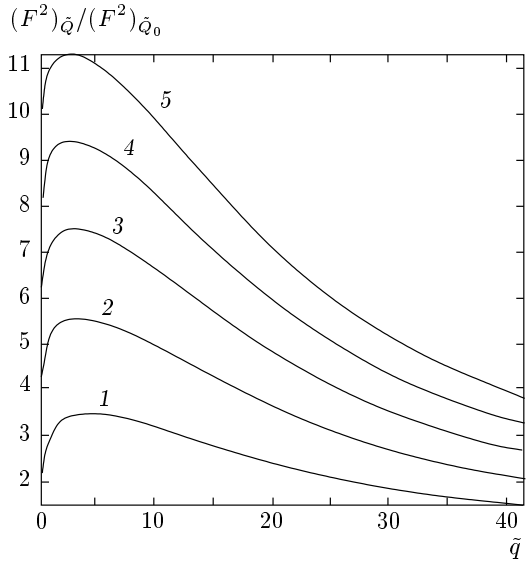

Fig. 7. Dependence of the ratio $(F_{\tilde{q}})^2/(F_{\tilde{q}_0})^2$ on the dimensionless phonon momentum for different time instants $t = 0.25$ (*1*), 0.5 (*2*), 0.75 (*3*), 1 (*4*), 1.25 (*5*) at $E = 33.6$ V/cm

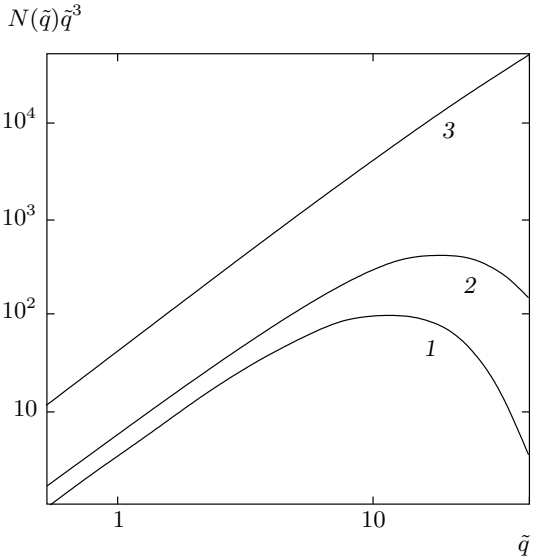

Fig. 8. Dependence of the phonon distribution function times the dimensionless phonon momentum cubed on the dimensionless electron momentum. Curve *1* and curve *2* refer to the respective equilibrium state at 20 K and 32 K. Curve *3* is for the phonon distribution function obtained as a result of numerical calculations for the electric field $E = 16$ V/cm at the instant $t = 2.5$

of the phonon distribution function in formula (17) and find the random force spectral density. Then we substitute this result in (16) and find

$$(Q_n)^2_\omega = \frac{(\chi/\pi)\hbar\omega(1/2 + N(\omega))}{m^2(\omega_n^2 - \omega^2)^2 + \chi^2\omega^2}. \tag{47}$$

Knowing $(Q_n)^2_\omega$, we calculate the correlation function $\psi(0)$ and its second derivative using formula (12):

$$\begin{aligned}
&\psi\,(0, N(\omega)) = \\
&= \lim_{\tau\to 0} \int\limits_{-\infty}^{\infty} \frac{(\chi/\pi)\hbar\omega(1/2+N(\omega))}{m^2(\omega_n^2-\omega^2)^2+\chi^2\omega^2}\, e^{-i\omega\tau}\, d\omega, \\
&\psi''\,(0, N(\omega)) = \\
&= -\lim_{\tau\to 0} \int\limits_{-\infty}^{\infty} \frac{(\chi/\pi)\hbar\omega^3(1/2+N(\omega))}{m^2(\omega_n^2-\omega^2)^2+\chi^2\omega^2}\, e^{-i\omega\tau}\, d\omega.
\end{aligned} \tag{48}$$

After that, we find $\Psi(\tau)$ and $\Psi''(0)$ using (10):

$$\Psi(0, N(\omega)) = 2\sum_{n=1}^{\bar{n}} \frac{q_n^2}{k^2}\psi\,(0, N(\omega))\,, \tag{49}$$

$$\Psi''(0, N(\omega)) = 2\sum_{n=1}^{\bar{n}} \frac{q_n^2}{k^2}\psi''\,(0, N(\omega))\,. \tag{50}$$

After substituting (9) in (1), we have the following relation that allows us to find $\delta\tilde{u}_{cr}^2$ when all other quantities are known:

$$\dot{\varepsilon}_d = bl\rho_d \frac{1}{2\pi}\sqrt{-\frac{\Psi''\,(0, N(\omega))}{\Psi\,(0, N(\omega))}} \times \exp\left\{-\frac{\delta\tilde{u}_{cr}^2}{2\Psi\,(0, N(\omega))}\right\}, \tag{51}$$

$$\delta\tilde{u}_{cr}\,(N(\omega)) = \sqrt{2\Psi\,(0, N(\omega))\ln\left(\frac{bl\rho_d}{2\pi\dot{\varepsilon}_d}\sqrt{-\frac{\Psi''\,(0, N(\omega))}{\Psi\,(0, N(\omega))}}\right)}. \tag{52}$$

Finally, we find σ from (11):

$$\sigma = \sigma_{cr}\left(1 - \frac{\delta\tilde{u}_{cr}(N(\omega))}{x_{cr}}\right), \tag{53}$$

$$\Delta\sigma\,(N(\omega)) = \sigma_{ext} - \sigma\,(N(\omega))\,. \tag{54}$$

The calculation results and experimental data were compared for nickel at the following values of experimental parameters: the applied external stress $\sigma_{ext} = 68.885$ MPa, $\dot{\varepsilon}_d = 1.19 \cdot 10^{-4}$ s^{-1}, $b = 3.52 \cdot 10^{-8}$ cm, and the product $l\rho_d = 435$ cm^{-1},

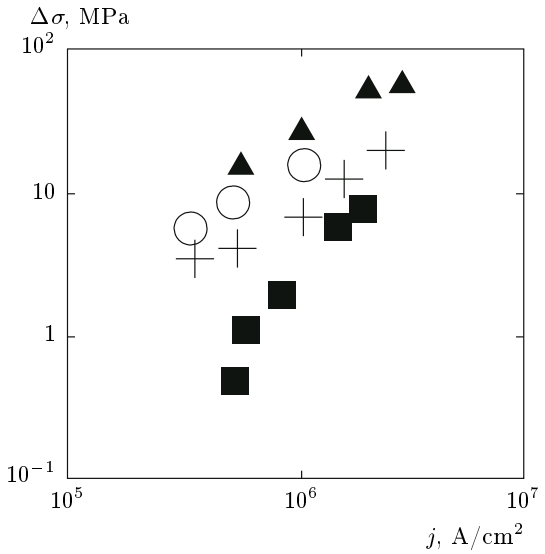

Fig. 9. Dependence of the loading drop $\Delta\sigma$ on the current density j. Squares are the experimental data provided by Troitsky [1]. Triangles correspond to the experiments of Lebedev [18]. Crosses correspond to our results based on the Granato–Lücke and Landau–Hoffman model with the phonon distribution function at the time instant $t = 2.5\mu$s for the electric field strengths 1.6, 2, 4, 8, 16 V/cm. Empty circles are the results for the instant $t = 15\mu$s for the electric field strength 1.6, 2, 4 V/cm

$U_0 = 3.34 \cdot 10^{-19}$ J, $x_{cr} = 0.2b$, $L = 3.5 \cdot 10^{-5}$ cm, and $B = 2 \cdot 10^{-10}$ N $\cdot$ s $\cdot$ cm^{02}.

Figure 9 clearly demonstrates that our approach gives results that are of the same order with experimental data. The expected loading drop in the case of heating under the conditions of thermodynamic equilibrium is several orders less that the loading drop observed in experiments. That is why we do not even put it on the figure. The loading drop that was calculated using the obtained data must be considered as a lower estimate because the time instants at which the calculation was finished are several times less than the current pulse duration in the experiments.

6. CONCLUSIONS

We have performed a kinetic analysis of nonequilibrium dynamics of the electron–phonon system of a crystal in a strong electric field. A method for numerically solving kinetic Boltzmann equations for the electron and phonon distribution function without expanding the electron distribution function in a series in the phonon energy is proposed. It has been shown that under the influence of a strong electric field, the electron distribution function becomes nonequilibrium in the vicinity of the Fermi energy and the influence of electron–phonon collisions becomes comparable to the influence of the field. The phonon distribution function is "heated" while remaining nonequilibrium in the region of long-wave phonons.

Basing on the Granato–Lücke and Landau–Hoffman model and using the calculated phonon distribution function, we have shown that the force of the action of the phonons on the dislocations is greater than it would be in the case of thermodynamic equilibrium at heating by 12 K. Previous results were defined more precisely. The conditions of the applicability of the Taylor expansion of the electron distribution function in the phonon energy depending on the temperature have been obtained.

This paper is financially supported in part by the National Academy of Sciences of Ukraine (grant №61-02-14) within the collaboration between the National Academy of Sciences of Ukraine and the Russian Foundation for Basic Research (grant №14-02-90248). We also express our gratitude to A. A. Parkhomenko for the valuable comments during the discussion of this work.

REFERENCES

1. V. I. Spitsyn and O. A. Troitskiy, *Elektroplasticheskaya Deformatsiya Metallov*, Nauka, Moscow (1985).

2. V. V. Stolyarov, Vestnik Nauchno-tehnicheskogo Razvitiya **67**, 35 (2013).

3. V. I. Karas and I. F. Potapenko, Voprosy Atomnoy Nauki i Tehniki. Seriya: Fizika Radiatsionnykh Povrezhdeniy i Radiatsionnoye Materialovedeniye **4–2**(62), 150 (2009).

4. V. E. Zakharov and V. I Karas, Physics-Uspekhi **56**, 49 (2013).

5. V. E. Zakharov, V. I. Karas, and A. M. Vlasenko, in *Proc. Int. Conf. MSS-14* "*Mode Conversion, Coherent Structures and Turbulence*", Lenand, Moscow (2014), p. 34.

6. V. I. Karas, A. M. Vlasenko, A. G. Zagorodny, and V. I. Sokolenko, in *Proc. Int. Conf. MSS-14* "*Mode Conversion, Coherent Structures and Turbulence*, Lenand, Moscow (2014), p. 64.

7. I. M. Neklyudov and N. V. Kamyshanchenko, *Fizicheskiye Osnovy Prochnosti i Plastichnosti Metallov.*

Chast 2: *Defekty v Kristallah*, Izd-vo Belgorodskogo GU, Moskva–Belgorod (1997).

8. A. I. Landau and Yu. I. Gofman, Fizika Tverd. Tela **16**, 3427 (1974).

9. A. Granato and K. Lücke, J. Appl. Phys. **27**, 583 (1956).

10. V. I. Dubinko, V. I. Karas, V. F. Klepikov, P. N. Ostapchuk, and I. F. Potapenko, Voprosy Atomnoy Nauki i Tehniki. Seriya: Fizika Radiatsionnyh Povrezhdeniy i Radiatsionnoye Materialovedeniye **4**–**2**(62), 158 (2009).

11. M. I. Kaganov, V. Ya. Kravchenko, and V. D. Natsik, Physics-Uspekhi **16**, 878 (1974).

12. N. Perrin and H. Budd, Phys. Rev. Lett. **28**, 1701 (1972).

13. F. G. Bass and Yu. G. Gurevich, *Goryachie Elektrony i Silnye Electromagnitnye Volny v Plasme Poluprovodnikov i Gazovogo Razryada*, Nauka, Moscow (1975).

14. V. P. Silin, *Vvedenie v Kineticheskuyu Teoriyu Gazov*, Librokom, Moscow, (2013).

15. E. M. Lifshits and L. P. Pitayevskiy, *Fizicheskaya Kinetika*, Fizmatlit, Moscow (2002).

16. V. I. Karas', I. F. Potapenko, and A. M. Vlasenko, Problems of Atomic Science and Technology. Series: Plasma Electronics and New Acceleration Methods **86**, 272 (2013).

17. V. I. Karas', A. M. Vlasenko, and V. I. Sokolenko, in *Abstracts of Proc.* 55^{th} *Int. Conf. Aktualniye Problemy Prochnosti*, NNTs KhFTI, Kharkov (2014), p. 14.

18. V. P. Lebedev and S. V. Savich, Visnyk KhNU, seriya "Fizika" **962**, 88 (2011).